Spin Fluctuations, Interband Coupling, and Unconventional Pairing in Iron-based Superconductors

Zi-Jian Yao,[1,2] Jian-Xin Li,[2,1] and Z. D. Wang[1]

[1] *Department of Physics and Center of Theoretical and Computational Physics, The University of Hong Kong, Pokfulam Road, Hong Kong, China*

[2] *National Laboratory of Solid State Microstructures and Department of Physics, Nanjing University, Nanjing 210093, China*

(Dated: December 13, 2008)

Based on an effective two-band model and using the fluctuation-exchange (FLEX) approach, we explore spin fluctuations and unconventional superconducting pairing in Fe-based layer superconductors. It is elaborated that one type of interband antiferromagnetic (AF) spin fluctuation stems from the interband Coulomb repulsion, while the other type of intraband AF spin fluctuation originates from the intraband Coulomb repulsion. Due to the Fermi-surface topology, a spin-singlet extended s-wave superconducting state is more favorable than the nodal d_{XY}-wave state if the interband AF spin fluctuation is more significant than the intraband one, otherwise vice versa. It is also revealed that the effective interband coupling plays an important role in the intraband pairings, which is a distinct feature of the present two-band system.

PACS numbers: 74.20.Mn, 74.20.Rp, 74.90.+n

The recent discovery of superconductivity with higher transition temperatures in the family of iron-based materials [1] has stimulated enormous research interests both experimentally [2, 3, 4, 5, 6, 7, 8, 9, 10, 11] and theoretically [12, 13, 14, 15, 16, 17, 18, 19, 20, 21, 22, 23]. In particular, the origin and nature of superconductivity and spin density wave (SDW) ordering observed in these materials have been paid considerable attention [2, 4, 9, 10, 11, 12, 14, 15, 17, 18, 22, 24]. Currently available experimental data suggested that the superconducting pairing state exhibit nodal behaviors [4], while preliminary theoretical arguements/analyses indicated the pairing possibilities of an extended s-wave (either without [14] or with nodes [15]), a nodal d-wave [15, 18], a spin-triplet s-wave [17], and a spin-triplet p-wave [21], all of them are based on the scenario that spin fluctuations induce the superconductivity in this kind of systems (with antiferromagnetic fluctuations being responsible for the former two spin-singlet pairings while ferromagnetic origin for the latter two spin-triplet pairings). Therefore, systematic and profound theoretical investigations on spin fluctuations and their relationship with the superconducting pairing are significant and of current interest.

This new family of superconductors has a layered structure, where the FeAs layer is experimentally suggested to be responsible for the superconductivity [1, 2, 3, 5, 6, 7, 8]. The LDA band calculations [12, 13, 24] indicate that there are five bands intersect the Fermi level in the folded Brillouin zone (BZ), in which four bands are quasi-two-dimensional. Therefore, in the representation of the unfolded (or extended) BZ, two bands may be able to reproduce the main features of the four Fermi pockets after folding. In this paper, we employ an effective two-band model Hamiltonian [20] to explore the low energy excitation physics including spin fluctuations and superconducting pairing with the FLEX approach [25]. It is illustrated that one type of commensurate AF spin fluctuations stems from the interband Coulomb repulsion associated with the nesting between the electron and hole Fermi pockets, while the other type of intraband AF spin fluctuation originates from the intraband Coulomb repulsion. Due to the Fermi-surface topology, a spin-singlet extended s-wave superconducting state is more favorable than the nodal d_{XY}-wave state as the interband spin fluctuation is significant, otherwise vice versa. It is also elaborated that the effective interband coupling is enhanced by the interband AF spin fluctuation and plays an important role in the intraband pairings.

We start from an effective two-band model Hamiltonian

$$H = H_0 + H_{int}, \tag{1}$$

where H_0 is given by

$$H_0 = \sum_{kl\sigma} \varepsilon_l(k) c^\dagger_{kl\sigma} c_{kl\sigma}. \tag{2}$$

Here $c_{kl\sigma}$ denotes the band-electron annihilation operator with the wave vector k, spin σ in the band l ($l = 1, 2$). In the present work, the two energy bands denote the hole band (band-1) and electron band (band-2), with their dispersions being approximated by $\varepsilon_{1,2}(k) = [\xi_{xz} + \xi_{yz} \mp \sqrt{(\xi_{xz} - \xi_{yz})^2 + 4\epsilon^2}]/2$, where $\xi_{xz}(k) = -2t_1 \cos k_x - 2t_2 \cos k_y - 4t_3 \cos k_x \cos k_y$, $\xi_{yz}(k) = -2t_2 \cos k_x - 2t_1 \cos k_y - 4t_3 \cos k_x \cos k_y$, $\epsilon(k) = -4t_4 \sin k_x \sin k_y$, as addressed in Refs. [20, 26]. Here, $\xi_{xz}(k)$ and $\xi_{yz}(k)$ may be understood as the iron d_{xz} and d_{yz} orbit-dispersions while $\epsilon(k)$ as the hybridization of the two orbits. To produce better the topology of the Fermi surface and band features of the LDA calculations [12, 13, 24], we set $t_1 = -1.0$, $t_2 = 1.5$, $t_3 = -1.2$, $t_4 = -0.95$, $\mu = 0.74$, 1.7

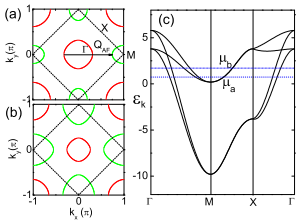

FIG. 1: (Color online) (a) and (b): The Fermi surfaces of the two-band model in the extended Brillouin zone (1 Fe per cell) for $\mu_a = 0.74$ and $\mu_b = 1.7$, where the thin dashed line denotes the folded Brillouin zone (2 Fe per unit cell) and the arrow represents the nesting wave vector (see text). (c) The corresponding band structure (energy is in the unit of t_1) in the folded Brillouin zone.

(in units of $|t_1|$), which gives rise to the electron Fermi pockets and the hole Fermi pockets (being respectively denoted by the green and red lines in Fig.1 (a)) as well as the band structure (Fig.1(c)).

The interacting term H_{int} consists of the effective intraband Coulomb interaction [27], $(U/2)\sum_{i,l,\sigma\neq\sigma'} c^\dagger_{il\sigma}c^\dagger_{il\sigma'}c_{il\sigma'}c_{il\sigma}$, the effective interband Coulomb interaction $(U'/2)\sum_{i,l\neq l',\sigma,\sigma'} c^\dagger_{il\sigma}c^\dagger_{il'\sigma'}c_{il'\sigma'}c_{il\sigma}$, the Hund's coupling $J\sum_{i,l\neq l',\sigma\sigma'} c^\dagger_{il\sigma}c^\dagger_{il'\sigma'}c_{il\sigma'}c_{il'\sigma}$, and the interband pair-hopping term $J'\sum_{i,l\neq l',\sigma\neq\sigma'} c^\dagger_{il\sigma}c^\dagger_{il\sigma'}c_{il'\sigma'}c_{il'\sigma}$, where the i-site is defined on the reduced lattice (one Fe per cell).

Experimental data [3, 9, 10, 11] indicated that the undoped material LaOFeAs behaves like a semimetal, and exhibits the itinerant antiferromagnetism. Thus it is reasonable to consider the Coulomb interaction to be intermediate in this system. In this sense, the FLEX approach [25] appears to be an adequate method. In this approach, the spin/charge fluctuations and the electron spectra are determined self-consistently by solving the Dyson's equation with a primary bubble- and ladder-type effective interaction. For the two-band system, the Green's function and the self-energy are expressed as the 2×2 matrices, satisfying the Dyson equation: $\hat{G(k)} = [i\omega_n\hat{I} - \hat{\varepsilon}(k) - \hat{\Sigma}(k)]^{-1}$, with $\varepsilon_{11} = \varepsilon_1$, $\varepsilon_{22} = \varepsilon_2$ and $\varepsilon_{12} = \varepsilon_{21} = 0$. The self-energy reads $\Sigma_{mn}(k) = \frac{T}{N}\sum_q\sum_{\mu\nu} V_{\mu m,\nu n}(q)G_{\mu\nu}(k-q)$, where the effective interaction $\hat{V}$ is a 4×4 matrix (with the basis ($|11\rangle$, $|22\rangle$, $|12\rangle$, $|21\rangle$)) given by [28]

$$V_{\mu m,\nu n}(q) = [\frac{3}{2}\hat{U}^s\hat{\chi}^s(q)\hat{U}^s + \frac{1}{2}\hat{U}^c\hat{\chi}^c(q)\hat{U}^c + \frac{3}{2}\hat{U}^s - \frac{1}{2}\hat{U}^c - \frac{1}{4}(\hat{U}^s+\hat{U}^c)\hat{\overline{\chi}}(\hat{U}^s+\hat{U}^c)]_{\mu m,\nu n}, \quad (3)$$

with

$$\hat{\chi}^s(q) = [\hat{I} - \hat{\overline{\chi}}(q)\hat{U}^s]^{-1}\hat{\overline{\chi}}(q),\ \hat{\chi}^c(q) = [\hat{I} + \hat{\overline{\chi}}(q)\hat{U}^c]^{-1}\hat{\overline{\chi}}(q) \quad (4)$$

as the spin and charge fluctuations. The irreducible susceptibility is $\overline{\chi}_{\mu m,\nu n}(q) = -\frac{T}{N}\sum_k G_{\nu\mu}(k+q)G_{mn}(k)$, and the interaction vertex reads,

$$\hat{U}^s = \begin{pmatrix} \hat{U}^{s1} & 0 \\ 0 & \hat{U}^{s2}\end{pmatrix}, \hat{U}^c = \begin{pmatrix} \hat{U}^{c1} & 0 \\ 0 & \hat{U}^{c2}\end{pmatrix}, \quad (5)$$

where $\hat{U}^{s1}_{mn} = U$ for $m = n$ and $2J$ otherwise, $\hat{U}^{s2}_{mn} = U'$ for $m = n$ and $2J'$ otherwise, $\hat{U}^{c1}_{mn} = U$ for $m = n$ and $2U' - 2J$ otherwise, $\hat{U}^{c2}_{mn} = -U' + 4J$ for $m = n$ and $2J'$ otherwise. In the above equations, $k \equiv (\mathbf{k}, \omega_n)$ and $q \equiv (\mathbf{q}, i\nu_n)$ are used, with ω_m the Matsubara frequency, T the temperature, and N the lattice site number.

The above equations form a closed set of equations and can be solved self-consistently to get the renormalized Green's function in the presence of the interaction H_{int}. After obtaining $\hat{G}(k)$, we can look into the superconducting instability and the gap symmetry from the following Eliashberg equation [28]

$$\lambda\Delta_{mn}(k) = -\frac{T}{N}\sum_q\sum_{\alpha\beta}\sum_{\mu\nu}\Gamma^{s,t}_{\alpha m,n\beta}(q) \times G_{\alpha\mu}(k-q)G_{\beta\nu}(q-k)\Delta_{\mu\nu}(k-q) \quad (6)$$

with the pairing potential being given by $\hat{\Gamma}^s(q) = \frac{3}{2}\hat{U}^s\hat{\chi}^s(q)\hat{U}^s - \frac{1}{2}\hat{U}^c\hat{\chi}^c(q)\hat{U}^c + \frac{1}{2}(\hat{U}^s + \hat{U}^c)$ and $\hat{\Gamma}^t(q) = -\frac{1}{2}\hat{U}^s\hat{\chi}^s(q)\hat{U}^s - \frac{1}{2}\hat{U}^c\hat{\chi}^c(q)\hat{U}^c + \frac{1}{2}(\hat{U}^s + \hat{U}^c)$ for the spin-singlet and spin-triplet states ($\hat{\Gamma}^t(q)$ is the same for the pairing spin projection $S_z = \pm 1, 0$), respectively. The eigenvalue $\lambda \to 1$ when the supercondcuting transition temperature T_c is reached. It is worth indicating that the interband Cooper pairing gap function Δ_{12} is decoupled from the equation of intraband Cooper pairing gap functions Δ_{ll} ($l = 1, 2$) and is vanishingly small for the present Fermi pockets pattern.

Numerical calculations are carried out with 32×32 k-meshes in the extended BZ and 1024 Matsubara frequencies. The analytic continuation to the real frequency is carried out with the usual Padé approximant. As for the interaction parameters, we note that a set of parameters with $U = 0.2 - 0.5$ bandwidth and $J \approx 0.09$ bandwidth was used in the literature [16]. Here we choose 8 sets of representative parameters: (U, U')=(6.5, 3.5) and (5.5, 4.0) for $J' = 1.0\,\&0.5$ and $\mu = 0.74\,\&1.7$ with $J = 1.0$.

Let us first address the static spin susceptibility $\chi^s(\omega = 0)$ ($\chi^c(\omega = 0) \ll \chi^s(\omega = 0)$, not shown here.). Fig.2 presents the physical spin susceptibility $\chi^s_{ph} = \sum_{mn}\chi^s_{mn,mn}$, its intraband components χ^s_{22}, χ^s_{11}, and the interband one χ^s_{12} in the extended BZ with $U = 6.5$, $U' = 3.5$, $J = J' = 1.0$, and $\mu = 0.74$. (For brevity, $\chi^s_{mn} \equiv \chi^s_{mn,mn}$ is used hereafter.) The physical spin susceptibility displays two sets of dominant peaks, with one around $(\pi, 0)$ and its symmetric points in the extended BZ, and the other around $(0.5\pi, 0.5\pi)$ and its symmetric points. The commensurate AF spin fluctuation around $(\pi, 0)$ comes from the interband Coulomb interaction associated with the nesting between the hole and electron

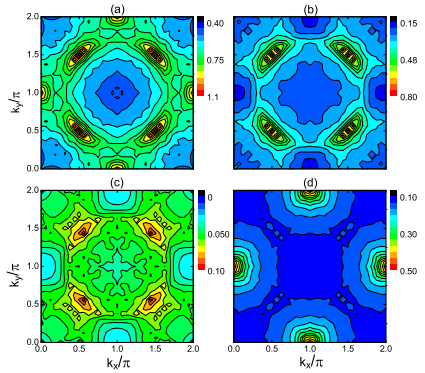

FIG. 2: (Color online) The k-dependence of the static spin susceptibility for $U = 6.5, U' = 3.5$, $J = J' = 1$, and $\mu = 0.74$ at temperature $T = 0.01$. (a) The physical spin susceptibility (see text). (b)-(d) The components of the spin susceptibility χ^s_{22}, χ^s_{11}, and χ^s_{12}, respectively.

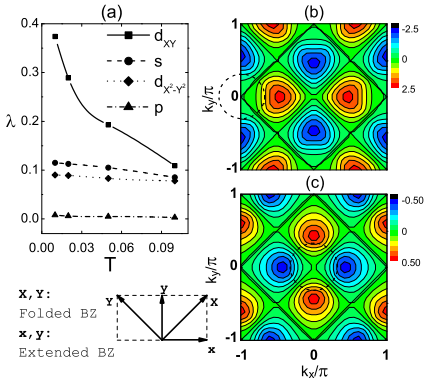

FIG. 3: (Color online) (a): Temperature dependence of the maximum eigenvalues, (b) and (c): k-dependence of the gap functions $\Delta_{2,1}(k)$ corresponding to the largest eigenvalue, for the same set of parameters as those in Fig.2 at temperature $T = 0.01$. The solid diamond is the folded BZ and the dashed circle denotes the Fermi pocket schematically.

pockets [18] (Fig.1 (a)), which is clearly seen from the interband component χ^s_{12} shown in Fig.2(d). The appearance of this type of AF spin fluctuation around $(\pm\pi, 0)$ and $(0, \pm\pi)$ is in good agreement with the neutron scattering measurements [10, 11], and here we refer to it as the interband AF spin fluctuation. More intriguingly, the other type of intraband spin fluctuation is seen to peak around $(0.5\pi, 0.5\pi)$ in the components χ^s_{11} and χ^s_{22}, which is mainly induced by the intraband Coulomb interaction U associated with the approximate nesting property within the renormalized Fermi pocket around the (π, π) point (not shown here). Notably, the peak position corresponds to $[0, \pi]$ (and $[\pi, 0]$) in the folded BZ and thus implies the emergence of a new component of "stripe"-type AF spin fluctuation in the primary lattice (with 2 Fe ions per unit cell), which could be referred to as the intraband spin fluctuation and may be detected directly by future neutron scattering experiments on single crystal samples.

The most favorable superconducting pairing symmetry at a fixed temperature is determined by solving the Eliashberg equation with the maximum eigenvalue. The calculated maximum eigenvalues (for various possible pairing symmetries) versus temperature are plotted in Fig.3(a). Firstly, one can see that the eigenvalue for the spin-triplet p-wave state is much smaller than those of the spin-singlet state, and at the mean time exhibits a flat temperature dependence. Therefore, we can safely rule out the possibility of the spin-triplet state in the present model calculation. In the spin-singlet channel, the eigenvalue of d_{XY}-wave state is larger than that of the s-wave state, and in particular the former increases rather rapidly with decreasing temperature. In view of this tendency, although the maximum eigenvalue $\lambda = 1$ has not been reached yet, it is reasonable to consider the spin-singlet d_{XY}-wave to be the most favorable state in this set of parameters. The calculated k-space structure of the gap functions for both the electron and hole bands in the extended BZ are depicted in Figs.3(b) and (c), respectively. It is seen that the pairing symmetries in both bands are of d_{XY}-wave, namely, the gap function $\Delta_{ll}(\mathbf{k}) \approx \Delta^0_l \gamma_{l\mathbf{k}}$ with $\gamma_{l\mathbf{k}} \approx 2 \sin k_X \sin k_Y$, where (k_X, k_Y) is the wave vector denoted in the folded BZ. Interestingly, we note that the gap magnitude in the electron-band is significantly larger than that in the hole-band. This feature could also be understood as follows. Eq.(6) may approximately be rewritten as

$$\lambda \Delta^0_l = \sum_{l'} K_{ll'} \Delta^0_{l'} \tag{7}$$

for $\omega = 0$, where $K_{ll'} = \sum_{\mathbf{k},\mathbf{k}'} \tilde{V}_{ll'}(\mathbf{k} - \mathbf{k}')$ with the effective intraband pairing potential and interband coupling as $\tilde{V}_{ll'} = -|G_{l'l'}|^2[(U^2 + 4J^2)\chi^s_{ll'}\delta_{ll'} + 4U'J'\chi^s_{ll'}(1 - \delta_{ll'})]\gamma_{l\mathbf{k}}\gamma_{l'\mathbf{k}'}/(N\sum_{\mathbf{k}} \gamma^2_{l\mathbf{k}})$. Since $K_{22} \gg K_{11}$ (mainly due to the result $\chi^s_{22} \gg \chi^s_{11}$), the gap amplitude of electron band (band 2) is mainly determined from the intraband pairing of itself, while that of the hole-band depends mainly on the interband coupling from the electron band. From the expression of $\tilde{V}_{ll'}$, it is elucidated that the intraband spin AF fluctuation leads to the intraband pairings, while the interband AF spin fluctuation enhances the effective interband coupling (associated with the interband coupling factor $U'J'$) and thus the intraband pairings of both bands [29]. The above conclusions are unchanged for $\mu = 1.7$ or $J' = 0.5$, where the intraband spin fluctuation has an even more impact on the pairing. However, if the interband AF spin fluctuation is dominant over the intraband one, as seen in Fig.4(a) for $U = 5.5$, $U' = 4.0$, $J = J' = 1$, and $\mu = 0.74$, an extended s-wave state (Figs.4 (b) and (c)) would be more favorable than the d-wave one. A similar conclusion has also be obtained in a recent renormaliztion group study [30].

Because the spin fluctuation χ^s is stronger than the

charge fluctuation χ^c (not shown here), the pairing interaction in the spin-singlet channel is positive ($\hat{\Gamma}^s(q) > 0$). Consequently, once the gap function satisfies the condition $\Delta_l(\mathbf{k})\Delta_{l'}(\mathbf{k}+\mathbf{Q}) < 0$, where $\mathbf{Q}$ is the wave-vector around which the pairing interaction peaks, we are able to obtain the largest eigenvalue solution of the Eliashberg equation. Focusing merely on the interband AF spin fluctuation, the above condition leads to two candidates of pairing symmetry on the singlet channel. One is the extended s-wave, with the gap function of each Fermi pocket having the same sign, while changing the sign between the electron and hole pockets, as shown in Fig.4(b) and (c). The other is the d-wave as shown in Fig.3(b) and (c). Actually, which one is more favored depends mainly on the existence of the intraband spin fluctuation caused by the Coulomb interaction U. For a larger U and the approximate nesting within the renormalized Fermi pocket, this spin fluctuation that peaks at $(0.5\pi, 0.5\pi)$ emerges (see Fig.2(b) and (c)), which leads to the gap function to change its sign within each Fermi pocket and thus induces a nodal d_{XY}-wave pairing. In contrast, if the intraband Coulomb interaction U is relatively weak, such that the intraband spin fluctuation is not significant, the extended s-wave state would energetically be favored as it opens a full gap around the Fermi pockets [31]. We think that this kind of connection between the peak structure of the spin response and the pairing symmetry established here is useful for probing the superconducting pairing symmetry by measuring the k-dependence of spin fluctuations in neutron scattering.

Finally, we note that the LDA energy bands in this system exhibits a more complex structure [12, 14, 15]. In the present two-band model, the d_{xz} and d_{yz} orbitals are chosen as these two orbitals have the largest weights to the energy bands crossing the Fermi level [32]. While, the d_{xy} orbital contributes also a weight to the energy band along the $\Gamma - M$ direction [32], and particularly in the unfolded Brillouin zone one of the hole Fermi pockets is displaced from the $(0,0)$ point to the (π,π) point as depicted in Figs.1(a) and (b), which is actually different from that in a more realistic energy band structure [15]. However, we wish to indicate that these two deficiencies do not affect meaningfully the nesting properties of the Fermi pockets, and thus the results/conclusions obtained above are still unchanged, at least qualitatively.

In summary, based on an effective two-band model and using the fluctuation-exchange approach, we have investigated spin fluctuations and superconductivity as well as the interband coupling in iron-based layered superconductors. We have elaborated that one type of commensurate AF spin fluctuation comes from the interband Coulomb interaction associated with the nesting between the hole and electron Fermi pockets, while the other type of intraband AF spin fluctuation originates from the intraband Coulomb repulsion. We have elucidated that, if the interband AF spin fluctuation plays a significant role, this fluctuation leads to the pairing with the spin-singlet extended s-wave being the most favorable state. Otherwise, the pairing is mainly determined by the intraband AF spin fluctuation, with d_{XY}-wave symmetry.

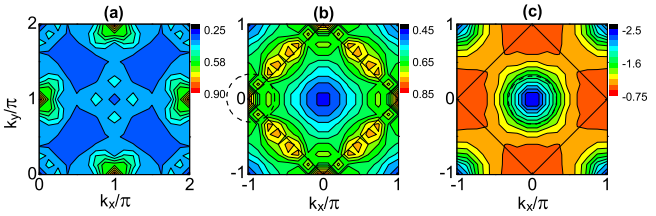

FIG. 4: (Color online) (a): The physical spin susceptibility, (b) and (c): k-dependence of the gap functions $\Delta_{2,1}(k)$ corresponding to the largest eigenvalue, for $U = 5.5, U' = 4.0$, $J = J' = 1.0$, and $\mu = 0.74$ at temperature $T = 0.01$.

Note added–(i) Recently, we note that the angle-resolved photoemission spectroscopy measurement on the (Ba,K)Fe_2As_2 superconductor [33] indicated the presence of nodeless gaps, which might imply the interband spin fluctuation plays likely a dominant role at least in these iron-based superconductors. (ii) After the work was posted on the e-Print archive, we note a similar work done by X.-L. Qi *et al* in [34].

We thank F.C. Zhang, Q. Han, Y. Chen, X. Dai, Z. Fang, T. K. Ng, Q. H. Wang, H. H. Wen, and S. C. Zhang for many helpful discussions. The work was supported by the NSFC (10525415 and 10429401), the RGC grants of Hong Kong (HKU-3/05C), the 973 project (2006CB601002,2006CB921800), and the Ministry of Education of China (Grants No.NCET-04-0453).

[1] Y. Kamihara, T. Watanabe, M. Hirano, and H. Hosono, J. Am. Chem. Soc. **130**, 3296 (2008).
[2] H. H. Wen, G. Mu, L. Fang, H. Yang, and X. Zhu, EPL **82**, 17009 (2008).
[3] Y. Kamihara *et al.*, Nature **453**, 376 (2008).
[4] L. Shan *et al*, EPL **83**, 57004 (2008); G. Mu *et al*, Chin. Phys. Lett. **25**, 2221 (2008).
[5] X. H. Chen *et al.*, Nature **453**, 761 (2008).
[6] G. F. Chen *et al.*, Phys. Rev. Lett. **100**, 247002 (2008).
[7] Z. A. Ren *et al.*, Materials Research Innovations **12**, 105, (2008).
[8] Z. A. Ren *et al.*, Chin. Phys. Lett. **25**, 2215 (2008).
[9] J. Dong *et al.*, EPL **83**, 27006 (2008).
[10] Clarina de la Cruz *et al.*, Nature **453**, 899 (2008).
[11] M. A. McGuire *et al.*, arXiv:0804.0796 (2008).
[12] D. J. Singh and M. H. Du, Phys. Rev. Lett. **100**, 237003 (2008).
[13] G. Xu *et al.*, EPL **82**, 67002 (2008).
[14] I. I. Mazin, D.J. Singh, M.D. Johannes, and M.H. Du, Phys. Rev. Lett. **101**, 057003 (2008).
[15] K. Kuroki *et al.*, Phys. Rev. Lett. **101**, 087004 (2008).
[16] C. Cao, P. J. Hirschfeld, and H. P. Cheng, Phys. Rev. B **77**, 220506(R) (2008).

[17] X. Dai, Z. Fang, Y. Zhou and F. C. Zhang, Phys. Rev. Lett. **101**, 057008 (2008).
[18] Q. Han, Y. Chen, and Z. D. Wang, EPL **82**, 37007 (2008); arXiv:0803.4346 (2008).
[19] M. M. Korshunov and I. Eremin, Phys. Rev. B **78**, 140509(R) (2008).
[20] S. Raghu, X. L. Qi, C. X. Liu, D. J. Scalapino, and S. C. Zhang, Phys. Rev. B **77**, 220503(R) (2008).
[21] P. A. Lee and X. G. Wen, Phys. Rev. B **78**, 144517 (2008).
[22] Z. Y. Weng, arXiv:0804.3228 (2008).
[23] F. Ma, Z.Y. Lu, and T. Xiang, arXiv:0804.3370 (2008).
[24] Z. P. Yin *et al.*, Phys. Rev. Lett. **101**, 047001 (2008).
[25] N. E. Bickers and D. J. Scalapino, Ann. Phys. (N.Y.) **193**, 206 (1989); Z.-J. Yao, J.-X. Li, and Z. D. Wang, Phys. Rev. B **76**, 212506 (2007).
[26] S. Graser *et al.*, Phys. Rev. B **77**, 180514(R) (2008).
[27] The effective interaction strengths (U, U', J, J') used here are not equal to those defined in the orbital representation.
[28] T. Takimoto, T. Hotta, and K. Ueda, Phys. Rev. B **69**, 104504 (2004).
[29] For example, when $J' = 0.5$, the gap magnitudes of both bands decrease.
[30] Fa Wang *et al.*, arXiv:0807.0498 (2008).
[31] We note that due to the essentially similar hole and electron Fermi pockets in the present model and that in Ref. 19, similar interband spin fluctuation peaks are observed, which was also thought to be relavent to the occurrence of the extended s-wave pairing in Ref. 19.
[32] L. Boeri *et al.*, Phys. Rev. Lett. **101**, 026403 (2008).
[33] H. Ding *et al.*, EPL **83**, 47001 (2008).
[34] X.-L. Qi *et al.*, arXiv:0804.4332 (2008).